Available online at www.sciencedirect.com
ScienceDirect
Journal of Molecular Structure 834–836 (2007) 445–453
Journal of MOLECULAR STRUCTURE
www.elsevier.com/locate/molstruc

Mössbauer, FT-IR and FE SEM investigation of iron oxides precipitated from $FeSO_4$ solutions

Marijan Gotić *, Svetozar Musić

Division of Materials Chemistry, Ruđer Bošković Institute, P.O. Box 180, HR-10002 Zagreb, Croatia

Received 4 September 2006; accepted 28 October 2006
Available online 30 January 2007

Abstract

Mössbauer and Fourier transform infrared (FT-IR) spectroscopies and thermal field emission scanning electron microscopy (FE SEM) were used to investigate the precipitation of iron oxides from $FeSO_4$ solutions. The hydrolysis of urea at 90 °C was utilized as a generator of OH^- ions needed for the precipitation of iron oxides. The formation of specific iron oxyhydroxide or oxide phase depended on the concentration of $FeSO_4$ and urea, as well as on the rate of oxygenation. In dependence on the experimental conditions different iron oxide phases, such as goethite, hematite and magnetite were found in the precipitates. Mössbauer spectra showed only the formation of substoichiometric magnetite ($Fe_{3-x}O_4$). Significant spectral differences in the RT Mössbauer spectrum of goethite phase were observed, and the spectra showing the presence of this phase could be fitted only taking into account the distribution of hyperfine magnetic fields. FE SEM inspection showed varying sizes and geometrical shapes of goethite particles. Goethite particles were elongated along the crystallographic *c*-axis.

Keywords: Goethite; Hematite; Magnetite; Mössbauer; FT-IR; FE SEM

1. Introduction

Iron oxides (a group name for oxyhydroxides and oxides) have found important applications as pigments, catalysts, gas sensors, magnetic materials, etc. These compounds are also important from the scientific point of view, due to their application as model systems in colloid and surface sciences. For that reason the syntheses and characterisations of *iron oxides* have been extensively investigated. Iron oxides undergo various phase transformations in aqueous media or in the solid state. The hydrolysis reactions and dissolution/reprecipitation mechanisms are dominant in aqueous media, whereas topotatic rearrangements are more typical of solid-state reactions.

The precipitation from aqueous $FeSO_4$ solutions can be used in the syntheses of iron oxides, such as α-FeOOH (goethite), γ-FeOOH (lepidocrocite), δ-FeOOH (feroxyhyte), α-Fe_2O_3 (hematite) and Fe_3O_4 (magnetite). However, these precipitations are very sensitive to experimental conditions, which may influence the phase composition, crystallinity, stoichiometry, size and geometrical shape of iron oxide particles. Musić et al. [1,2] have found that the phase composition of iron oxides precipitated from $FeSO_4$ solutions strongly depended on the $[Fe^{2+}]/[OH^-]$ concentration ratio at the beginning of the precipitation process, on the rate of oxygenation, the time of precipitation, the temperature and the kind of alkali added (NH_4OH or NaOH). Lorenz et al. [3] investigated the phase composition of precipitates obtained from $FeSO_4$, $FeCl_2$ or $FeBr_2$ solutions by the oxidation of Fe^{2+} ions with O_2 in alkaline pH media, and found that goethite was the dominant phase in the precipitates. Also, the size of goethite particles obtained from $Fe(OH)_2$ suspension by air oxidation, strongly depended on the reaction time [4]. Kiyama et al. [5] monitored the growth of needle-like goethite particles precipitated from the $FeSO_4$

* Corresponding author.
E-mail address: gotic@irb.hr (M. Gotić).

0022-2860/$ - see front matter © 2006 Elsevier B.V. All rights reserved.
doi:10.1016/j.molstruc.2006.10.059

solution by air oxidation at 40 °C. Acicular goethite particles can be utilized in the production of acicular maghemite (γ-Fe_2O_3) particles which exhibit specific magnetic properties. Anantharaman et al. [6] investigated optimal experimental conditions for the formation of maghemite from goethite. Lepidocrocite was synthesized [7] from 0.36 M $FeSO_4$ solution at 20 °C and pH 7. Synthetic feroxyhyte can be synthesized [8,9] by (a) very rapid bubbling of O_2 through a suspension of $Fe(OH)_2$, (b) rapid oxidation of $Fe(OH)_2$ by H_2O_2, or (c) exposure of dried $Fe(OH)_2$ to O_2. Gotić et al. [10] have found that strong alkalinity of mother liquor was an important factor for feroxyhyte formation via the $Fe(OH)_2$ precursor. The best crystallinity of feroxyhyte was obtained when the synthesis was conducted in a completely inert atmosphere. Šubrt et al. [11,12] investigated the precipitation of hematite from $FeSO_4$ solutions. Kiyama [13] investigated conditions for the synthesis of magnetite by the air oxidation of $Fe(OH)_2$ suspensions. Matsuda [14] synthesized magnetite utilizing reactions between β-FeOOH and $FeSO_4$ in an aqueous solution containing urea at 98 °C.

In continuation of an earlier work [15] we are focusing on the capabilities of Mössbauer and FT-IR spectroscopies in the characterisation of iron oxides formed in precipitation processes. The application of FE SEM microscopy made possible to inspect the size and geometrical shape of iron oxide particles and investigate a possible influence of these factors on the corresponding Mössbauer spectra.

2. Experimental

2.1. Preparation of samples

The chemicals $FeSO_4{\cdot}7H_2O$ and urea were of analytical purity. Twice-distilled water was prepared in own laboratory. Finely grained $FeSO_4{\cdot}7H_2O$ salt was kept in an oxygen-free atmosphere to inhibit Fe^{2+} oxidation to Fe^{3+}. Precipitations were performed in the reaction glass flask fitted with four inlet necks. A water-cooled reflux condenser was mounted onto the reaction vessel. A glass stirrer was rotated by a small electromotor and the angular speed of the stirrer was measured. The reaction vessel was isolated from the glass mixer by a specially designed adapter filled with silicon oil. Air was cleaned with a series of in-line filters between the air compressor and the reaction vessel. Air flow rate was adjusted to commercial valves and flowmeters. After 6 h of precipitation the chemical reactions were stopped and the precipitates were separated from the mother liquor by centrifugation. The precipitates were subsequently washed with twice-distilled water, then dried. Experimental conditions for the synthesis of samples are given in Table 1.

2.2. Instrumentation

^{57}Fe Mössbauer spectra were recorded in the transmission mode using standard instrumental configuration by WISSEL (Starnberg, Germany). The ^{57}Co in the rhodium matrix was used as a Mössbauer source. The spectrometer was calibrated at RT using the spectrum of a standard α-Fe foil. The velocity scale and all the data refer to the metallic α-Fe absorber at RT. The experimentally observed Mössbauer spectra were fitted using the *MossWinn* program.

FT-IR spectra were recorded at RT using a Perkin-Elmer spectrometer, model 2000. The FT-IR spectrometer was linked to a personal computer loaded with the IRDM (IR Data Manager) program to process the recorded spectra. The specimens were pressed into small discs using a spectroscopically pure KBr matrix. Mössbauer and FT-IR measurements were checked by the X-ray diffraction of isolated precipitates.

Thermal field emission scanning electron microscope (FE SEM, model JSM-7000F) manufactured by JEOL Ltd. was used. FE SEM was linked to an EDS/INCA 350 (energy dispersive X-ray analyser) manufactured by Oxford Instruments Ltd. Samples were not coated with a conductive layer, and the accelerating voltage was kept low.

Table 1
Experimental conditions for the preparation of samples at 90 °C

Sample	Volume of solution (ml)	$FeSO_4$ (mol dm^{-3})	Urea (mol dm^{-3})	Time of precipitation (h)	Time of aeration (h)	Flow rate (l min^{-1})	Speed of stirrer (rpm)	Final pH
S1	200	0.1	0.5	6	6	0.4	250	3.20
S2	200	0.1	1.5	6	6	0.4	250	5.38
S3	200	0.1	3	6	6	0.4	250	7.80
S4	200	0.1	6	6	6	0.4	250	8.20
S5	200	0.1	10	6	6	0.4	250	8.45
S6	200	0.1	0.5	6			250	4.30
S7	200	0.1	1.5	6			250	5.67
S8	200	0.1	3	6			250	5.98
S9	200	0.1	6	6			250	6.28
S10	200	0.1	0.5	6	6	0.4	250	2.25
S11	200	0.1	1.5	6	6	0.4	250	4.00

3. Results and discussion

3.1. Mössbauer spectroscopy

Samples S1–S5 were precipitated from 0.1 M $FeSO_4$ solutions containing urea with varying initial concentration from 0.5 to 10 M. At elevated temperature urea undergoes hydrolysis in line with the chemical reaction

$$(NH_2)_2CO + H_2O \rightarrow 2NH_3 + CO_2 \quad (1)$$

thus serving as a generator of OH^- ions,

$$NH_3 + H_2O \rightarrow NH_4OH \quad (2)$$

Mother liquors separated from the precipitation suspensions S1–S5 showed a pH change from 3.20 to 8.45. The corresponding precipitates formed at these pH values showed varying phase composition, as indicated by Mössbauer spectra in Figs. 1 and 2 and Mössbauer parameters in Table 2. The raw spectrum of sample S1 can be considered as the superposition of one sextet with very broadened spectral lines and one paramagnetic doublet. With a view to obtaining a good fit we resolved the above-mentioned sextet of goethite into two subsextets. The outer sextet gave $B_{hf} = 38.5$ T, whereas the inner sextet, which was fitted taking into account the distribution of hyperfine magnetic field, gave an average $B_{hf} = 28.7$ T. Precipitated goethites often take this shape of the Mössbauer spectrum. A well-crystalline goethite is characterised by one sextet of spectral lines at RT and intensity ratios 3:2:1:1:2:3. However, the spectral lines of goethite are as a rule broadened and deviate from the theoretical intensity ratios 3:2:1:1:2:3. In the case of very fine goethite particles, one paramagnetic doublet at RT can be obtained. For example, goethite particles smaller than ~15–20 nm show a superparamagnetic type of the Mössbauer spectrum at RT. Goethite particles smaller than 8 nm show a superparamagnetic type of the Mössbauer spectrum down to 77 K [16]. Taking into account the RT Mössbauer spectrum of sample S1 and a corresponding XRD pattern, the presence of small paramagnetic doublet can be assigned to a small fraction of very fine goethite particles. XRD pattern of sample S1 showed only the presence of a goethite phase. In the spectrum of sample S2 the additional hyperfine magnetic splitting component is

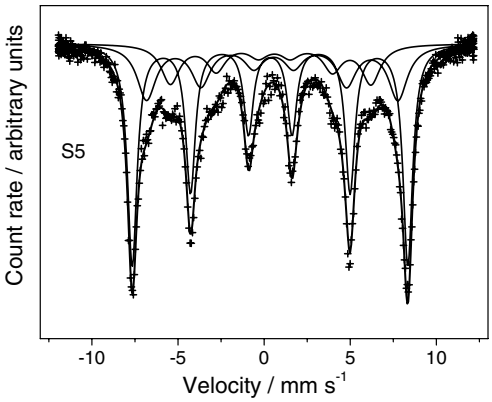

Fig. 2. ^{57}Fe Mössbauer spectra of samples S5, recorded at RT.

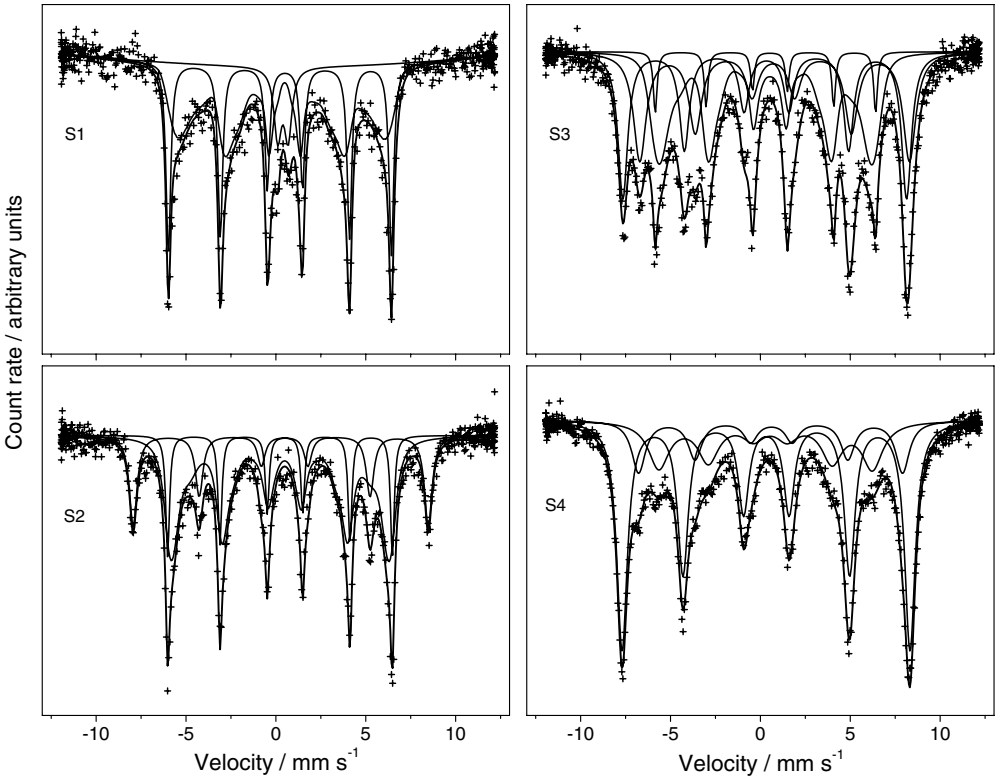

Fig. 1. ^{57}Fe Mössbauer spectra of samples S1–S4, recorded at RT.

Table 2
^{57}Fe Mössbauer parameters at RT calculated for sample S1–S11

Sample	Fitting procedure	δ (mm s^{-1})	Δ or E_Q (mm s^{-1})	B_{hf} (T)	Γ(mm s^{-1})	Area (%)	Phase composition	Phase fraction
S1	PD	0.39	0.58		0.50	8.1		0.08
	G1	0.41	−0.17	28.7	0.31	55.8	Goethite	0.92
	G2	0.36	−0.28	38.5	0.32	36.2		
S2	G1	0.37	−0.25	34.5	0.65	61.1	Goethite	0.79
	G2	0.36	−0.27	38.8	0.25	17.7		
	H	0.38	−0.22	50.9	0.50	21.1	Hematite	0.21
S3	G1	0.41	−0.24	33.8	0.50	37.5	Goethite	0.43
	G2	0.40	−0.25	38.0	0.25	5.6		
	M1	0.29	−0.10	49.0	0.66	28.7	Magnetite	0.57
	M2	0.76	0.07	46.5	0.85	28.2		
S4	M1	0.32	−0.01	49.7	0.72	58.2	Magnetite	0.76
	M2	0.59	−0.05	45.5	0.92	17.4		
	G2	0.42	−0.26	36.9	1.39	24.4	Goethite	0.24
S5	M1	0.35	−0.02	49.6	0.68	54.8	Magnetite	0.82
	M2	0.51	−0.09	45.3	1.33	27.6		
	G2	0.49	−0.21	36.1	1.29	17.6	Goethite	0.18
S6	G1	0.40	−0.27	34.6	0.58	63.1	Goethite	0.87
	G2	0.37	−0.26	38.9	0.23	23.8		
	H	0.39	−0.25	51.1	0.44	13.0	Hematite	0.13
S7	PD	0.47	0.44		0.27	1.7		0.02
	G1	0.44	−0.22	34.3	0.55	29.2	Goethite	0.45
	G2	0.36	−0.26	38.4	0.27	15.6		
	M1	0.32	−0.04	49.6	0.52	32.4	Magnetite	0.53
	M2	0.68	−0.13	45.3	1.20	21.0		
S8	M1	0.32	−0.00	49.7	0.53	45.5	Magnetite	0.68
	M2	0.58	−0.06	46.1	1.03	22.1		
	G1	0.48	−0.25	33.5	0.53	25.0	Goethite	0.32
	G2	0.35	−0.26	38.2	0.27	7.4		
S9	PD	0.40	0.58		0.35	2.4		0.02
	M1	0.35	−0.03	49.5	0.56	47.7	Magnetite	0.73
	M2	0.46	−0.07	45.7	1.05	25.3		
	G2	0.41	−0.28	36.7	0.9	24.6	Goethite	0.25
S10	PD	0.38	0.60		0.53	22.0		0.22
	G1	0.37	−0.15	27.5	0.66	78.0	Goethite	0.78
S11	G1	0.41	−0.26	33.2	0.44	74.7	Goethite	1.00
	G2	0.39	−0.25	38.6	0.27	25.3		

Key: δ = isomer shift given relative to α-Fe at RT; Δ or E_Q = quadrupole splitting; B_{hf} = hyperfine magnetic field; Γ = line width.
Error: $\delta = \pm 0.01$ mm s^{-1}; Δ or $E_Q = \pm\ 0.01$ mm s^{-1}; $B_{hf} = \pm 0.2$ T.
Remarks: PD = paramagnetic doublet; G1 = introduced goethite subsextet fitted to the distribution of hyperfine magnetic fields; G2 = introduced goethite subsextet fitted without the distribution of hyperfine magnetic fields; M1 = outer sextet of magnetite; M2 = inner sextet of magnetite; H = sextet of hematite.

observed which is characterised by $B_{hf} = 50.9$ T. This B_{hf} value is smaller than that of a well-crystallized hematite ($B_{hf} = 51.8$ T; [1]). The effect of a decreased B_{hf} value can be assigned to the decreased crystallinity of precipitated hematite particles and/or their substructure. The substructure of precipitated hematite particles may consist of very fine particles/crystallites as building units [17]. The Mössbauer spectrum of sample S3 indicated the presence of goethite and a substoichiometric magnetite ($Fe_{3-x}O_4$). The goethite component was considered a distribution of hyperfine magnetic fields and in this sense it was fitted with two subsextets, similar as in the case of sample S1. The phase fractions of goethite and substoichiometric magnetite in sample S1, obtained by Mössbauer spectroscopy, are close to 1:1 and in line with the semiquantitative XRD analysis. Samples S4 (Fig. 1) and S5 (Fig. 2) showed the presence of goethite and substoichiometric magnetite. In the case of these samples the goethite component was fitted with one sextet taking into account the distribution of hyperfine magnetic fields.

Fig. 3 shows the Mössbauer spectra of samples S6–S9. The precipitation of these samples was taken under more reductive conditions, i.e., there was no bubbling of air. The fitting approach was the same as in the earlier cases. At the initial concentration of 0.5 M urea the mixture of goethite and hematite precipitated, whereas at higher initial concentrations of urea goethite and substoichiometric magnetite precipitated, with a tendency of increasing the molar fraction of $Fe_{3-x}O_4$.

Fig. 4 shows the Mössbauer spectra of samples S10 and S11. These samples were precipitated from 0.3 M $FeSO_4$ solutions under aeration conditions given in Table 1. Sample S10 showed the superposition of one collapsing sextet and a paramagnetic doublet, whereas sample S11 showed one sextet with broadened spectral lines, which can be assigned to goethite. XRD patterns of samples S10 and

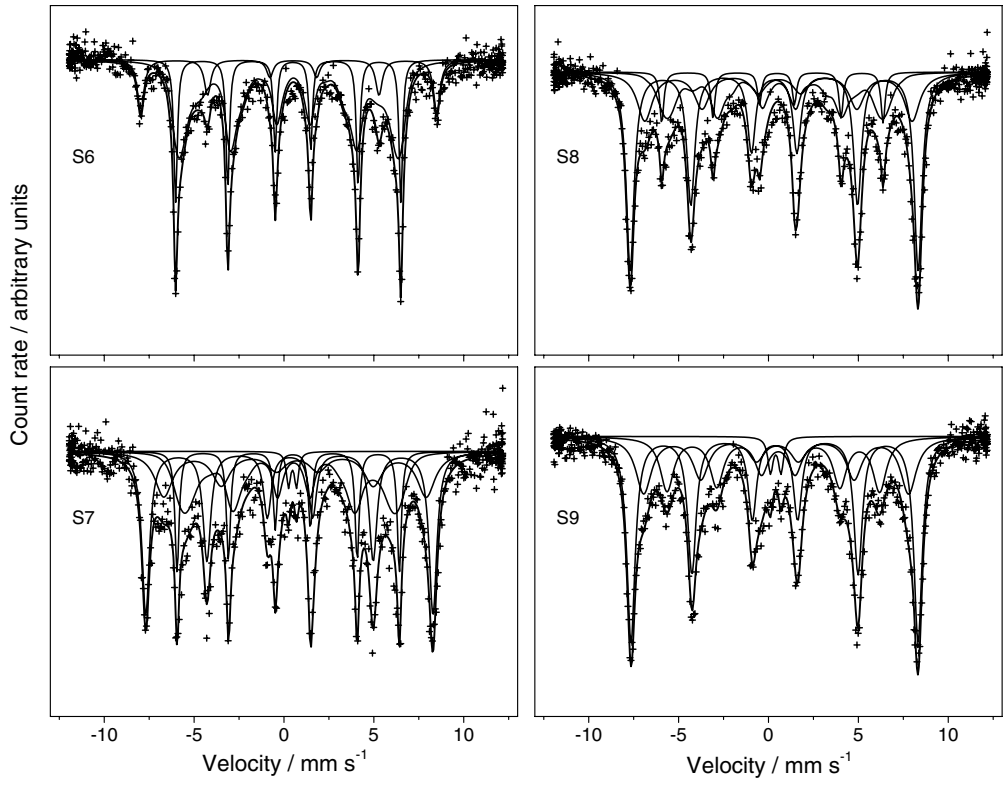

Fig. 3. ^{57}Fe Mössbauer spectra of samples S6–S9, recorded at RT.

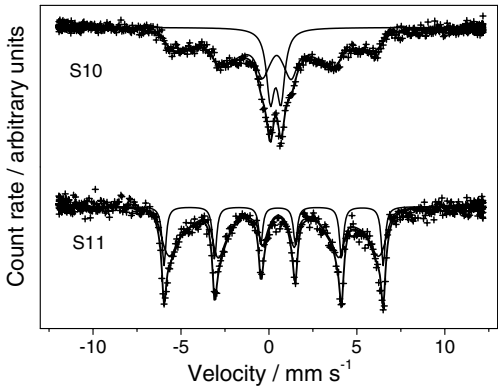

Fig. 4. ^{57}Fe Mössbauer spectra of samples S10 and S11, recorded at RT.

S11 correspond to goethite as a single phase in both samples.

3.2. FT-IR spectroscopy

Fig. 5 shows the FT-IR spectra of samples S1–S5. The FT-IR spectrum of sample S1 shows two broad bands at 3455 and 3144 cm^{-1}. The IR band at 3455 cm^{-1} can be assigned to the stretching modes of surface H_2O molecules or to an envelope of hydrogen-bonded surface OH groups. The IR band at 3144 cm^{-1} can be assigned to the OH stretching mode in the goethite structure. The IR band at 1643 cm^{-1} is close to the position of H_2O bending vibrations. A smaller-intensity bands at 1193 and 1126, can be

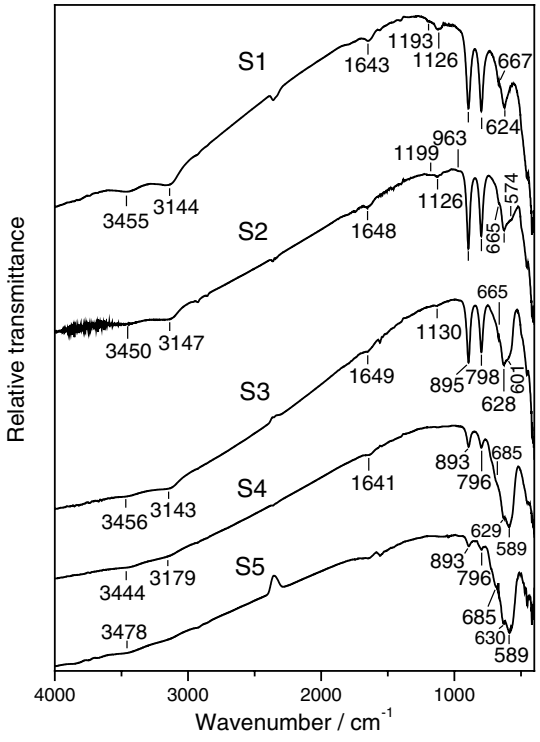

Fig. 5. Fourier transform infrared spectra of samples S1–S5, recorded at RT.

assigned to specifically adsorbed sulphate groups [18]. At acidic pH values an increased adsorption of sulphate groups on iron oxide surfaces occurs, which decreases with

an increased pH. Two prominent IR bands at 895 and 798 cm^{-1} are due to Fe–O–H bending vibrations in goethite. In accordance with works by Verdonck et al. [19] and Cambier [20], the IR band at 624 cm^{-1} can be assigned to Fe–O stretching vibrations. The position of this IR band was also related to the shape of goethite particles. The FT-IR spectrum of sample S2 showed similar spectral features of goethite. The presence of a shoulder at 574 cm^{-1} can be related to the presence of hematite, as shown by Mössbauer and XRD pattern. Iglesias and Serna [21] reported the IR spectrum of hematite. Hematite spheres showed IR bands at 575, 485, 385 and 360 cm^{-1}. Aggregation and matrix effects [22], as well as the crystallinity effect [23] on the IR spectrum of hematite, were also reported.

The FT-IR spectra of samples S3–S5 showed typical Fe–O–H bending bands of goethite, whereas the shoulder at 601 and the band at 589 cm^{-1} can be assigned to an increased amount of substoichiometric magnetite in these samples. The FT-IR spectrum of substoichiometric magnetite $Fe_{2.91}O_4$ showed two IR bands at 586 and 404 cm^{-1} [24]. Ishii et al. [25] assigned the IR bands at 565 and 360 cm^{-1} to the $\nu_1(F_{1u})$ and ν_2 (F_{1u}) vibration modes in Fe_3O_4. The positions of these two bands depend on the stoichiometry of magnetite. Also, the specifically adsorbed sulphate groups were diminishing in order S3–S5 due to an increased pH, while sulphate groups were absent from sample S5.

The FT-IR spectra of samples S6–S9 are shown in Fig. 6. The spectrum of sample S6 shows very strong and sharp bands at 894 and 799 cm^{-1} typical of goethite, whereas the shoulder at 571 cm^{-1} can be assigned to the presence of hematite as an associated phase, which is in line with the Mössbauer results. The intensive IR band at 590/587 cm^{-1} recorded for samples S7–S9 can be assigned to the substoichiometric magnetite, in line with previous discussion.

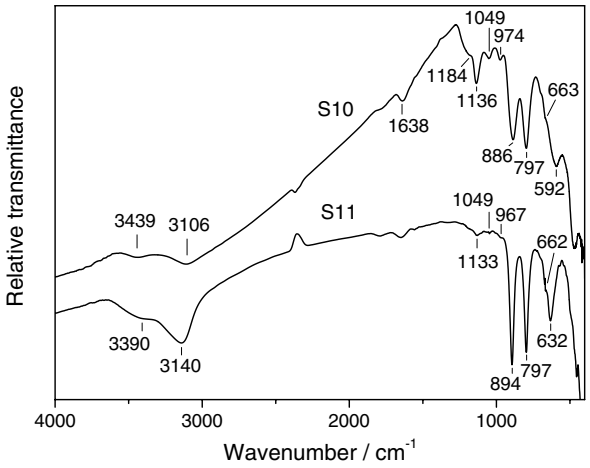

Fig. 7. Fourier transform infrared spectra of samples S10 and S11, recorded at RT.

The FT-IR spectra of samples S10 and S11 (Fig. 7) can be assigned to goethite as a single phase. On the basis of IR bands at 1184, 1136, 1049 and 974 cm^{-1} it can be inferred that sample S10 contains a significant amount of specifically adsorbed sulphate groups, which occupy external as well as internal surfaces in goethite particles. The final pH of the mother liquor of sample S10 was 2.25. Sample S11 showed less adsorbed sulphates, which is in accordance with the final pH of precipitation at 4.40.

3.3. FE SEM

All samples were inspected by FE SEM. Characteristic results are given in Figs. 8–11. Fig. 8 shows the FE SEM

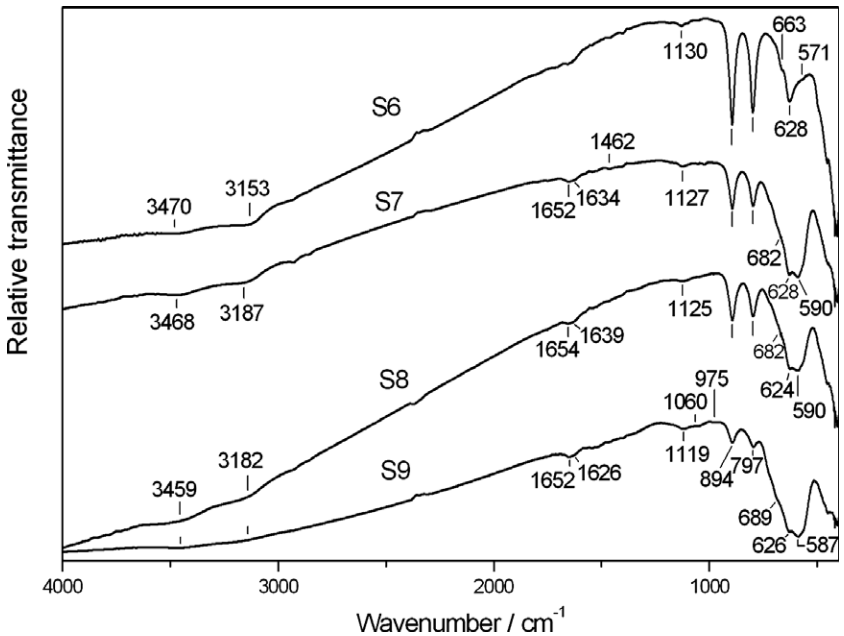

Fig. 6. Fourier transform infrared spectra of samples S6–S9, recorded at RT.

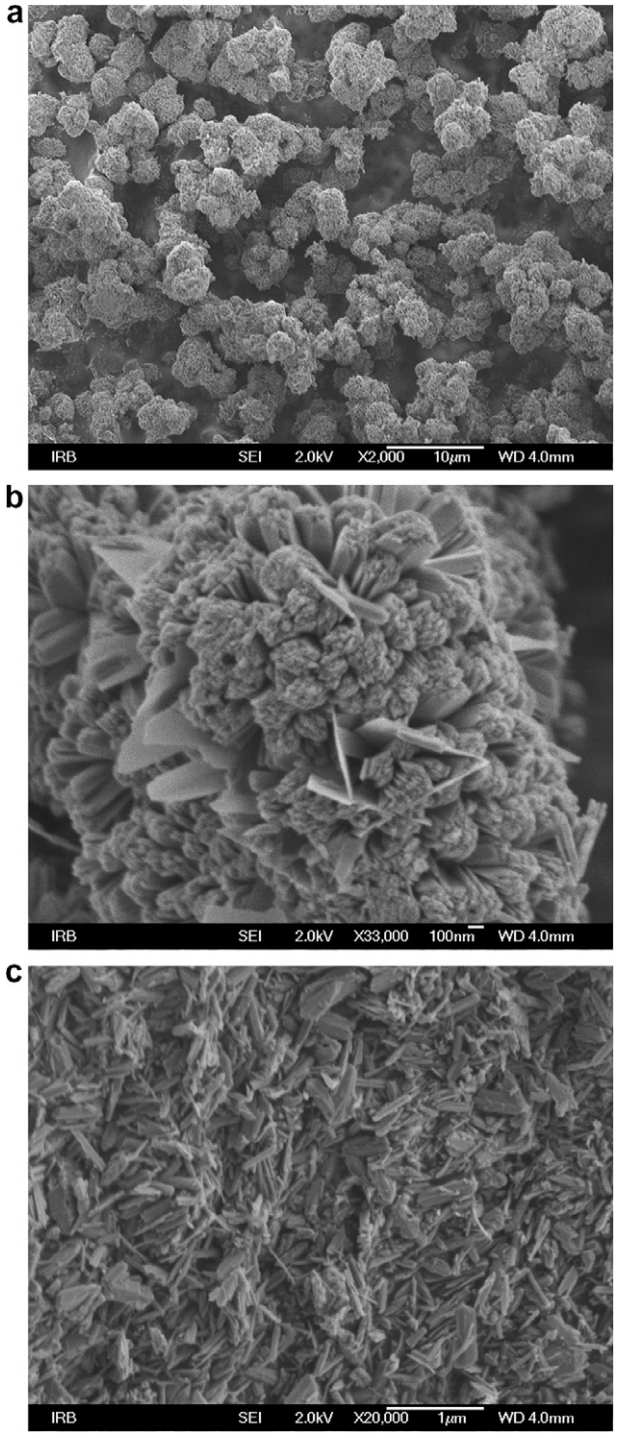

Fig. 8. FE SEM micrographs of sample S1 (two details (a and b)) and sample S11 (c).

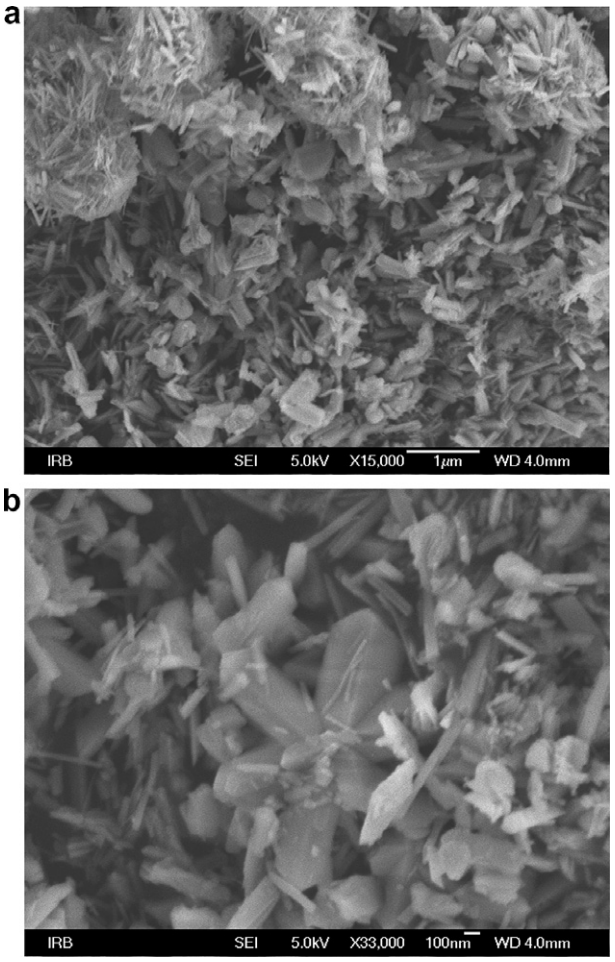

Fig. 9. FE SEM micrographs of sample S6.

micrographs of sample S1 (two details; (a and b)) and sample S11 (one detail); (c). All previous analyses have confirmed that these samples contain goethite as a single phase. Fig. 8a shows that goethite particles are actually the aggregates of much smaller particles. Fig. 8b shows one such aggregate under much higher optical magnification. It is well visible that this goethite aggregate consists of (a) bundles of rods, (b) big thin rods and (c) plate-like particles which are possibly broken parts of big thin rods. The diameter of goethite rods aggregated into bundles is ~20–35 nm, whereas the thickness of plate-like particles is 20–40 nm. Sample S11 (Fig. 8c) also showed a variety of sizes and shapes of goethite particles. Goethite particles in sample S1 and S11 were elongated along the crystallographic *c*-axis, which was also typical of other samples containing the goethite phase, for example sample S6 (Fig. 9a). The formation of dendritic microstructure in the same sample is also visible (Fig. 9b). These micrographs support the conclusion that the corresponding RT Mössbauer spectra are influenced by the size and shape of goethite particles. A certain effect of decreased crystallinity on the Mössbauer spectrum of goethite in the samples cannot be excluded. FE SEM results confirmed that the fitting procedure used in the analysis of the recorded Mössbauer spectra was realistic.

Magnetite particles were in the form of aggregates (Fig. 10a; sample S5), and they showed a tendency to form big magnetite particles through the aggregation process (Fig. 10b; sample S8, central particle). Fig. 10c shows a detail obtained for sample S8 under high optical magnification (100,000×). In the central part of this micrograph

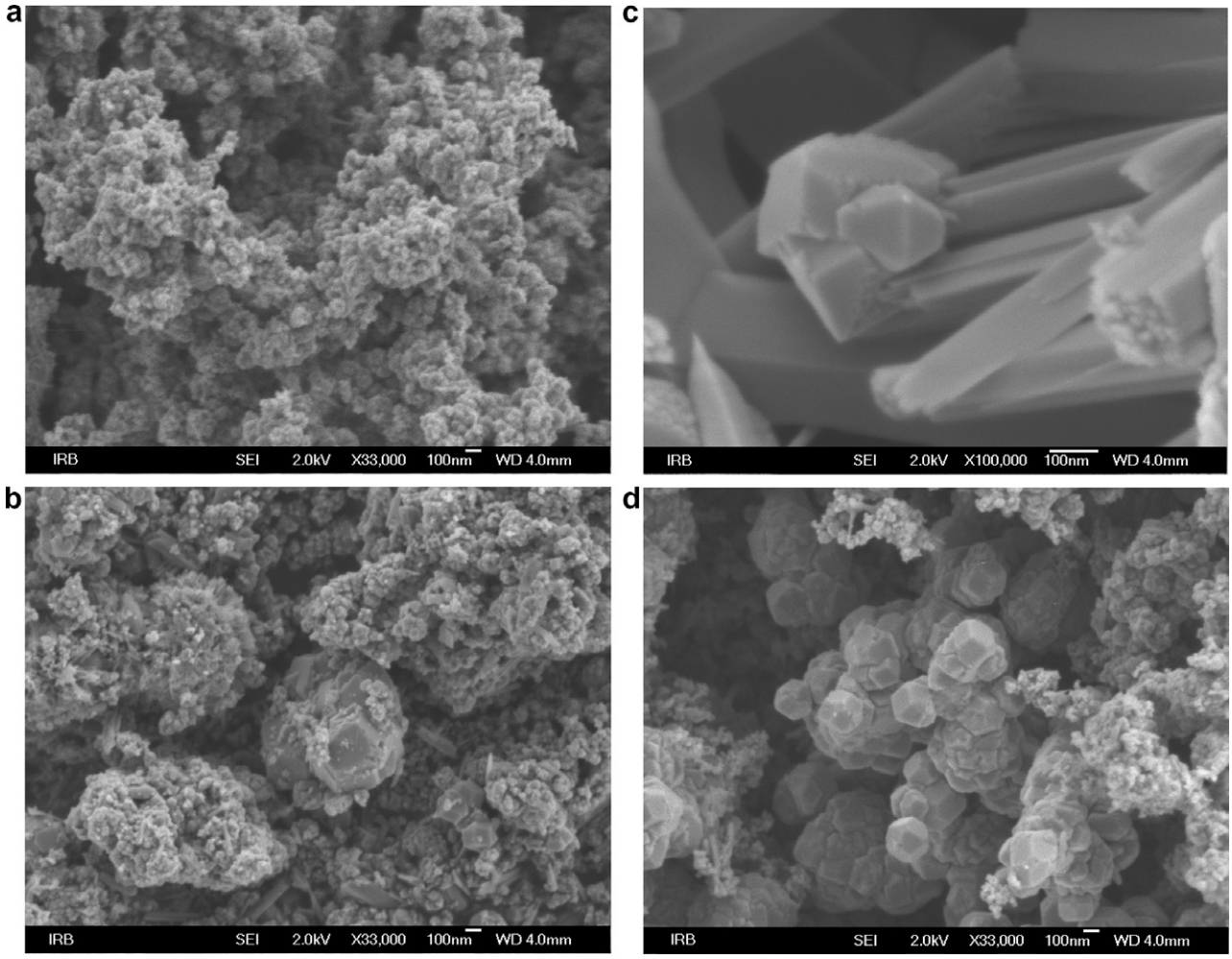

Fig. 10. FE SEM micrographs of sample S5 (a), sample S8 (two details; (b and c)) and sample S9 (d).

(Fig. 10c), the aggregation of octahedral magnetite particles is well visible. In the same micrograph rod-like goethite particles are present. This micrograph shows a bundle of goethite rods of nanosize diameter in the frame of thin goethite plate-like rods. Fig. 10d shows magnetite particles of various dimensions formed by (i) the mechanism of crystal growth in the suspension, and (ii) the aggregation process. A small fraction of goethite rods is also noticed in the same micrograph. Fig. 11 shows the FE SEM micrographs of sample S10 (two details; (a and b)). It is visible that the near spherical aggregates (Fig. 11a) consist of very fine particles of about 5–10 nm in size (Fig. 11b).

4. Conclusion

- Iron oxides were precipitated at 90 °C from $FeSO_4$ solutions containing urea. Urea undergoes hydrolysis at 90 °C, thus serving as a generator of OH^- ions. The phase composition of precipitates depended on experimental conditions of the precipitation process. By changing the conditions of aeration of the precipitation systems, more oxidative or reductive conditions could be achieved.
- Goethite, hematite and magnetite were found in the precipitates. Mössbauer spectra showed only the formation of substoichiometric magnetite ($Fe_{3-x}O_4$) in the investigated samples. The Mössbauer spectrum of the goethite phase showed spectral differences, and the corresponding spectra could be well-fitted only taking into account the distribution of hyperfine magnetic fields. FT-IR spectroscopy showed specifically adsorbed sulphates on iron oxides precipitated at more acidic pH values. The adsorption of sulphates decreased with an increased pH.
- FE SEM inspection showed varying sizes and geometrical shapes of goethite particles, as well as their tendency towards aggregation. Also, goethite particles were elongated along the crystallographic *c*-axis. Size, geometrical shape and possibly a lower crystallinity were considered as the factors which influenced the Mössbauer spectrum of goethite. The aggregation effect played an important role in the formation of big magnetite particles, whereas

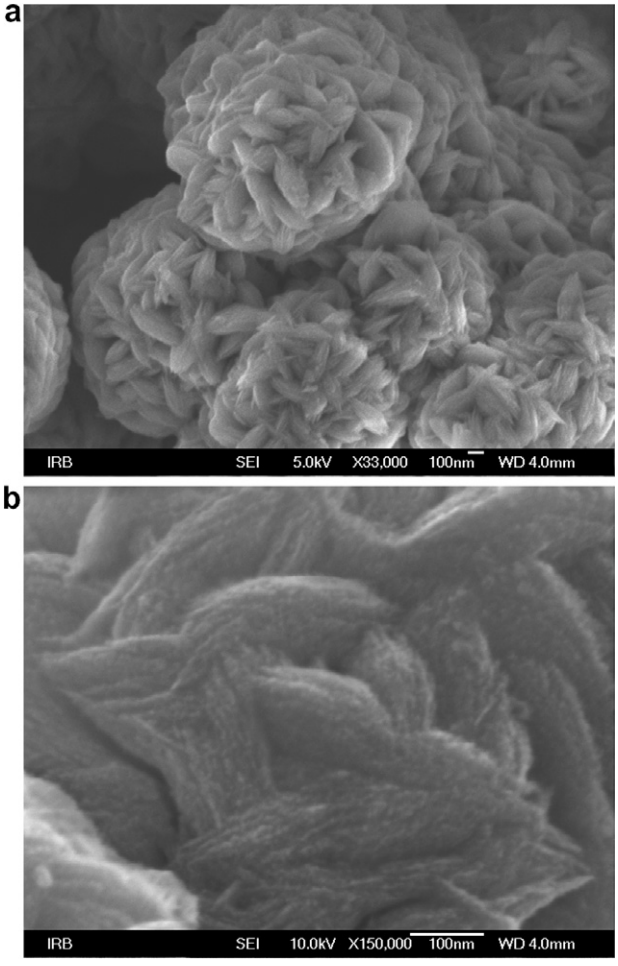

Fig. 11. FE SEM micrographs of sample S10 (two details (a and b)).

in dependence on the experimental conditions the mechanism of crystal growth of magnetite in the suspension could be dominant.

References

[1] S. Musić, I. Czakó-Nagy, S. Popović, A. Vértes, M. Tonković, Croat. Chem. Acta 59 (1986) 833.
[2] S. Musić, S. Popović, M. Gotić, Croat. Chem. Acta 60 (1987) 661.
[3] M. Lorenz, S. Knake, K. Stopperka, J. Signal AM 10 (1982) 449.
[4] M. Feige, M. Lorenz, K. Stopperka, J. Signal AM 8 (1980) 357.
[5] M. Kiyama, S.-I. Shamoto, N. Horiishi, Y. Okuda, T. Takada, Bull. Inst. Chem. Res. Kyoto Univ. 64 (1986) 150.
[6] M.R. Anantharaman, S. Seshan, S.N. Shringi, H.V. Keer, Bull. Mater. Sci. 6 (1984) 59.
[7] A. Šolcova, A. Šubrt, F. Hanousek, P. Holba, V. Zapletal, J. Lipka, Silikaty 24 (1980) 133.
[8] W. Feitknecht, Z. Electrochem. 63 (1959) 34.
[9] O. Muller, R. Wilson, W. Krakow, J. Mater. Sci. 14 (1997) 2929.
[10] M. Gotić, S. Popović, S. Musić, Mater. Lett. 21 (1994) 289.
[11] J. Šubrt, F. Hanousek, V. Zapletal, H. Štepankova, J. Mater. Sci. 17 (1982) 215.
[12] J. Šubrt, A. Šolcova, F. Hanousek, A. Petrina, V. Zapletal, Coll. Czech. Chem. Commun. 49 (1984) 2478.
[13] M. Kiyama, Bull Chem. Soc. Jpn. 47 (1974) 1646.
[14] K. Matsuda, Nippon Kagaku Kaishi 11 (1983) 1589.
[15] S. Musić, S. Popović, M. Gotić, J. Mater. Sci. 25 (1990) 3186.
[16] E. Murad, J.H. Johnston, Iron oxides and oxyhydroxides, in: G.J. Long (Ed.), Mössbauer Spectroscopy Applied to Inorganic Chemistry, Plenum Publishing Corporation, New York, 1987, pp. 507–582.
[17] M. Ristić, S. Musić, M. Godec, J. Alloys Comp. 417 (2006) 292.
[18] S. Musić, A. Šarić, S. Popović, K. Nomura, T. Sawada, Croat. Chem. Acta 73 (2000) 541.
[19] L. Verdonck, S. Hoste, F.F. Roelandt, G.P. Van der Kelen, J. Mol. Struct. 79 (1982) 273.
[20] P. Cambier, Clay Miner. 21 (1986) 191.
[21] J.E. Iglesias, C.J. Serna, Miner. Petrogr. Acta 29A (1985) 363.
[22] J.E. Iglesias, M. Ocaña, C.J. Serna, Appl. Spectr. 44 (1990) 418.
[23] Sh. Yariv, E. Mendolovici, Appl. Spectr. 33 (1979) 410.
[24] M.S. Ellid, Y.S. Murayed, M.S. Zoto, S. Musić, S. Popović, J. Radioanal. Nucl. Chem. 258 (2003) 299.
[25] M. Ishii, M. Nakahira, T. Yamanaka, Solid State Commun. 11 (1972) 209.